Higher Order Chimera Grid Interface for Transonic Turbomachinery Applications

Petr Straka

Abstract In this paper a higher-order accuracy chimera mesh interface for transonic flow in linear turbine blade cascades is described. Proposed method for calculation of the flow in a transonic blade cascade is applied. Conservation of mass flux through the blade cascade is evaluated. Results of calculation are compared with experimental data.

Keywords Finite-volume method, chimera grid
MSC2010: 35L65, 76H05, 76F40, 65N08

1 Introduction

It is possible to cover a computational domain with structured mesh, even in cases of complex geometry, using the structured chimera mesh. In transonic turbomachinery applications, shock waves structures are formed. The interface between overlapped meshes must operate correctly even if the shock wave intersects. Using of standard interpolation methods (linear, bilinear, polynomial) as well as conservative interpolation methods proposed for subsonic flow [1–3] leads to non-physical reflections of the shock waves at the chimera mesh interface in the case of supersonic flow. A gradient limiting technique is used in this contribution for suppression of the non-physical reflection of shock wave at the chimera mesh interface.

Petr Straka
Aeronautical Research and Test Institute, Plc, Beranových 130, 199 05 Prague - Letňany, Czech Republic, e-mail: straka@vzlu.cz

J. Fořt et al. (eds.), *Finite Volumes for Complex Applications VI – Problems & Perspectives*, Springer Proceedings in Mathematics 4,
DOI 10.1007/978-3-642-20671-9_79,

2 Govering equation

The linear blade cascade is a simple model of an axial turbine stator or rotor wheel. Flow in the linear turbine blade cascade is modeled as 2D compressible viscous turbulent flow of perfect gas. This model is described by the Favre-averaged Navier–Stokes equation

$$\frac{\partial \mathbf{W}}{\partial t} + \frac{\partial \mathbf{F}_i}{\partial x_i} = \mathbf{Q}\,, \tag{1}$$

where $\mathbf{W} = [\rho,\ \rho u_1,\ \rho u_2,\ e]^{\mathrm{T}}$ is conservative variable vector, ρ is density, u_1 and u_2 are velocity vector components, e is total energy per unit volume, $\mathbf{F}_i = \mathbf{F}_i^{inv} - \mathbf{F}_i^{vis}$ $(i = 1,\ 2)$ stands for flux vectors and $\mathbf{Q}$ is source term. In our case is $\mathbf{Q} = \mathbf{0}$. System (1) is closed by two-equation TNT $k - \omega$ turbulence model [4] which can be formulated in vector form as follows:

$$\frac{\partial \mathbf{W}_t}{\partial t} + \frac{\partial \mathbf{F}_{t,i}}{\partial x_i} = \mathbf{Q}_t\,, \tag{2}$$

where $\mathbf{W}_t = [\rho k,\ \rho \omega]^{\mathrm{T}}$ is vector of turbulent quantities, k is turbulent kinetic energy, ω is specific dissipation rate, $\mathbf{F}_{t,i} = \mathbf{F}_{t,i}^{inv} - \mathbf{F}_{t,i}^{vis}$ $(i = 1,\ 2)$ are flux vectors of turbulent quantities and $\mathbf{Q}_t$ is production and dissipation source term for turbulent quantities.

3 Numerical solution method

The govering equations are discretized on the structured multiblock mesh with quadrilateral elements using a cell-centered finite-volume technique and solved through a time-marching scheme. Both, the mean flow and the turbulence equations are integrated over a control volume D_i and some area integrals are transformed into line integrals along its boundary ∂D_i by the Green-Gauss theorem. Thus

$$\int\int_{D_i} \frac{\partial \mathbf{W}}{\partial t}\,\mathrm{d}x_1\,\mathrm{d}x_2 + \oint_{\partial D_i} \mathbf{F}_n\,\mathrm{d}s = \int\int_{D_i} \mathbf{Q}\,\mathrm{d}x_1\,\mathrm{d}x_2\,, \tag{3}$$

where $\mathbf{F}_n = n_i\,\mathbf{F}_i/|\mathbf{n}|$ ($\mathbf{n} = [n_1,\ n_2]$ is the boundary outward normal vector). The line integrals take the following discrete forms

$$\oint_{\partial D_i} \mathbf{F}_n^{inv}\,\mathrm{d}s = \sum_{j=1}^{4} \Phi^{inv}(\mathbf{W}_j^L,\ \mathbf{W}_j^R,\ \mathbf{n}_j)\,s_j\,, \tag{4}$$

$$\oint_{\partial D_i} \mathbf{F}_n^{vis}\,\mathrm{d}s = \sum_{j=1}^{4} \Phi^{vis}(\mathbf{W}_j^C,\ (\nabla \mathbf{W})_{D_j^{dual}},\ \mathbf{n}_j)\,s_j\,. \tag{5}$$

In the mean flow equations, the inviscid numerical fluxes Φ^{inv} are computed by means of the Osher-Solomon flux splitting scheme [5]. Higher order accuracy is achieved through the 2D linear reconstruction method which will be discussed later. In eq. (4) $\mathbf{W}_j^L$ and $\mathbf{W}_j^R$ denote the *left* and *right* states in the corresponding Riemann problem [6]. In the turbulence equations, the inviscid numerical fluxes are computed by the first-order upwind flux-splitting scheme, based on the local convective velocity normal to the cell boundary. The numerical viscous fluxes Φ^{vis} are computed using second-order central scheme, where $\nabla\mathbf{W}$ is approximated through the Green-Gauss formula on a dual cell (Fig. 1) and the local conservative variables vector at the cell boundary is computed as $\mathbf{W}_j^C = (\mathbf{W}_j^L + \mathbf{W}_j^R)/2$.

The time integration is performed using first-order backward Euler scheme

$$\left(\mathbf{I} + \Delta t \, \frac{\partial \mathbf{R}_i^{low}}{\partial \mathbf{W}_i}\right) \Delta \mathbf{W}_i^{n+1/2} + \Delta t \sum_{j=1}^{4} \frac{\partial \mathbf{R}_i^{low}}{\partial \mathbf{W}_j} \Delta \mathbf{W}_j^{n+1/2} = -\Delta t \, \mathbf{R}_i^n \ , \qquad (6)$$

where $\Delta\mathbf{W}^{n+1/2} = \mathbf{W}^{n+1} - \mathbf{W}^n$, and residual approximation $\mathbf{R}_i$ is given as

$$\mathbf{R}_i = \frac{1}{|D_i|} \sum_{j=1}^{4} [\Phi^{inv}(\mathbf{W}_j^L, \ \mathbf{W}_j^R, \ \mathbf{n}_j) - \Phi^{vis}(\mathbf{W}_j^C, \ (\nabla\mathbf{W})_{D_j^{dual}}, \ \mathbf{n}_j)] \, s_j \ . \qquad (7)$$

$\mathbf{R}_i^{low}$ denotes first-order approximation in eq. (6).

3.1 Linear reconstruction technique

As mentioned above, higher order accuracy is achived through the 2D linear reconstruction method, which is used for extrapolation of state vector $\mathbf{W}$ at the cell boundary. A piecewise linear function is used for reconstruction of the components

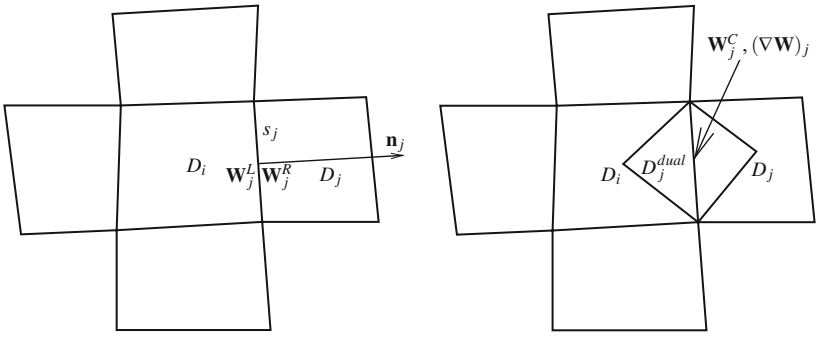

Fig. 1 Scheme of the structured quadrilateral mesh with dual volume

w_k ($k = 1, \ldots 4$) of vector $\mathbf{W}$

$$w_k = f_k(x_1, x_2) = a_k + b_k x_1 + c_k x_2. \tag{8}$$

Coefficients a_k, b_k and c_k are given by supposition

$$w_{k,l} = \frac{1}{|D_l|} \int \int_{D_l} f_k(x_1, x_2)\, \mathrm{d}x_1\, \mathrm{d}x_2, \tag{9}$$

where l denotes index of three neighbouring cells. We define four linear functions $f_k^1, \ldots, f_k^4$ for reconstruction of state vector components $w_{k\,\mathrm{C}}$ ($k = 1, \ldots 4$) from centre of cell denoted C (Fig. 2) to centre of boundary with cell denoted R, where index l in eq. (9) is for function f_k^1: $l = \mathrm{C, R}$ T, for function f_k^2: $l = \mathrm{C, T, L}$, for function f_k^3: $l = \mathrm{C, L, B}$ and for function f_k^4: $l = \mathrm{C, B, R}$ (R, T, L, B are designations of cells adjacent to cell C - Fig. 2). Components $w_{k,\,\mathrm{CR}}^L$ of reconstructed state vector $\mathbf{W}_{\mathrm{CR}}^L$ (where L means left side in outward normal direction) are given as

$$w_{k,\,\mathrm{CR}}^L = w_{k\,\mathrm{C}} + \delta_{k\,\mathrm{CR}}\,, \tag{10}$$

where $w_{k\,\mathrm{C}}$ are components of state vector in centre of cell C and $\delta_{k\,\mathrm{CR}}$ is defined as

$$\delta_{k\,\mathrm{CR}} = \delta_{k\,\mathrm{CR}}^{min}\, \psi(r(\delta_{k\,\mathrm{CR}}^{min}, \delta_{k\,\mathrm{CR}}^{max}))\,, \tag{11}$$

$$\delta_{k\,\mathrm{CR}}^{min} = \min_m \{f_k^m(x_{\mathrm{CR},1}, x_{\mathrm{CR},2}) - w_{k\,\mathrm{C}}\}\,,\ m = 1, \ldots, 4\,, \tag{12}$$

$$\delta_{k\,\mathrm{CR}}^{max} = \max_m \{f_k^m(x_{\mathrm{CR},1}, x_{\mathrm{CR},2}) - w_{k\,\mathrm{C}}\}\,,\ m = 1, \ldots, 4\,. \tag{13}$$

There is $r(\delta^{min}, \delta^{max}) = \delta^{max}/\delta^{min}$ and ψ stands for the limiting function enforcing monotonicity to the solution in eq. (11). The limiters of Van Albada, Van Leer and the super-bee limiter are used in this work.

$$\psi_{VA}(r) = \begin{cases} 0, & r \le 0\,, \\ (r^2 + r)/(r^2 + 1), & r > 0, \end{cases} \tag{14}$$

$$\psi_{VL}(r) = \begin{cases} 0, & r \le 0\,, \\ 2r/(r + 1), & r > 0, \end{cases} \tag{15}$$

$$\psi_{SB}(r) = \begin{cases} 0, & r \le 0\,, \\ 2r, & 0 \le r \le 1/2\,, \\ 1, & 1/2 \le r \le 1\,, \\ r, & 1 \le r \le 2\,, \\ 2, & r \ge 2\,. \end{cases} \tag{16}$$

3.2 Chimera grid interface

For numerical solution of flow in the turbine blade cascade, O-type mesh is used around the blade profile, H-type mesh covers the chanel between blades as shown in Fig. 3. For simple implementation of the chimera mesh the cells of mesh are classified into three categories: category C0 refers to the regular cell in which the conservative variables vector **W** is solved, category C1 refers to the hidden cell which is skiped during the solution procedure, category C2 refers to the interpolation cell in which the vector **W** is interpolated from overlapped mesh. The same method, as described in paragraph 3.1, is used for interpolation of state vector **W** into the centre of the cell type C2. We need to have state vector $\mathbf{W}^R$ for calculation of flux through boundary between cells type C0 and C2 (Fig. 4 left), which is obtained using the linear reconstruction in cell type C2. One can see, that for correct reconstruction of vector $\mathbf{W}^R$ at the boundary between cells type C0 and C2, we need to have two layers of interpolation cells type C2 (Fig. 4 right).

Proposed chimera mesh interface is very simple for implementation, is higher-order of accuracy and is robust for transonic flow calculation. The mass flux conservation error will be discussed later.

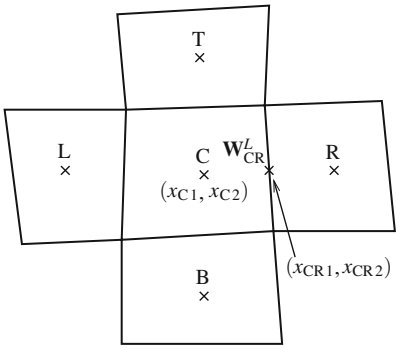

Fig. 2 Scheme of the linear reconstruction on the structured quadrilateral mesh

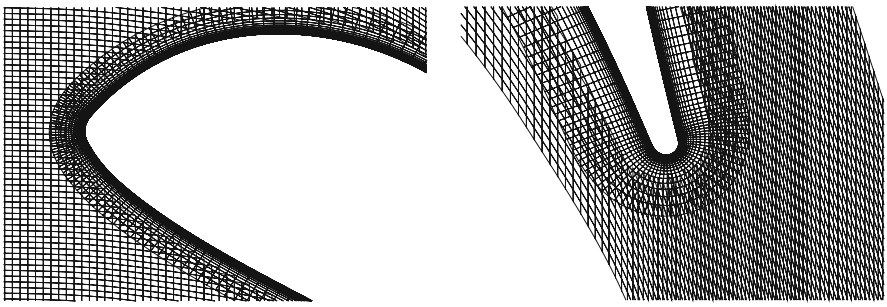

Fig. 3 Detail of chimera mesh around leading and trailing edge

4 Application

The numerical method described in sec. 3 is used for solution of flow in the linear transonic turbine blade cascade VS33R. The computational domain with set boundary conditions types is shown in Fig. 5 (left). The solution was calculated for isentropic output Mach number $0.5 < M_{is,out} < 1.3$, isentropic output Reynolds number $Re_{is,out} = 8.5 \times 10^5$, zero angle of attack and 2 % of inlet turbulence intensity. Transonic flow field in Mach number isolines form is shown in Fig. 5 right. Error of conservation of the mass flux through the blade cascade given as $(1 - q_{in}/q_{out}) \cdot 100$ (where q is the mass flux) is shown in Fig. 7. Further distribution of the total pressure loss coefficient $\eta = 1 - p_{tot,out}/p_{tot,in}$ is compared with the experimental data [7] in Fig. 6.

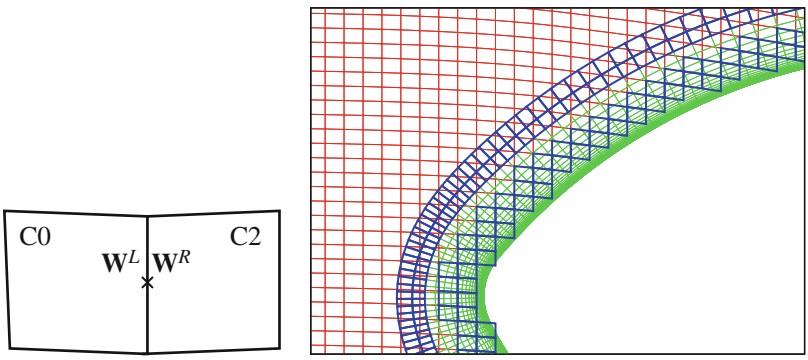

Fig. 4 Left: detail of interface between regular and interpolation cell. Right: two layers of interpolation cells of C2 type (blue)

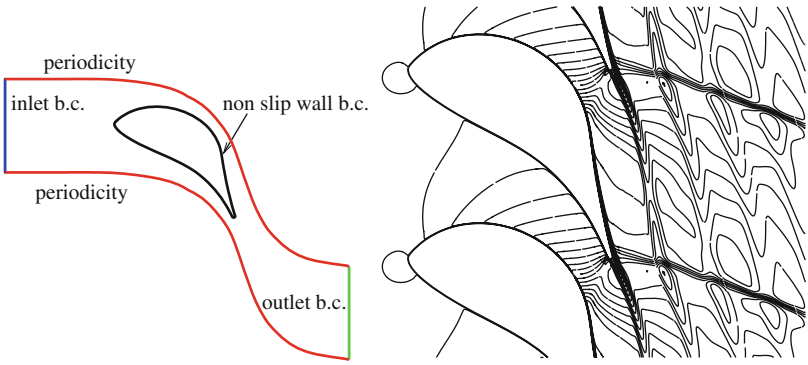

Fig. 5 Left: scheme of computational domain in linear blade cascade. Right: Mach number isolines ($M_{is,out} = 1.3$)

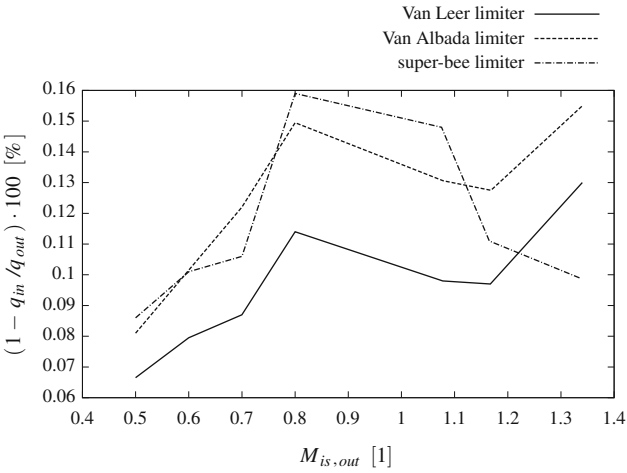

Fig. 6 Distribution of the mass flux conservation error

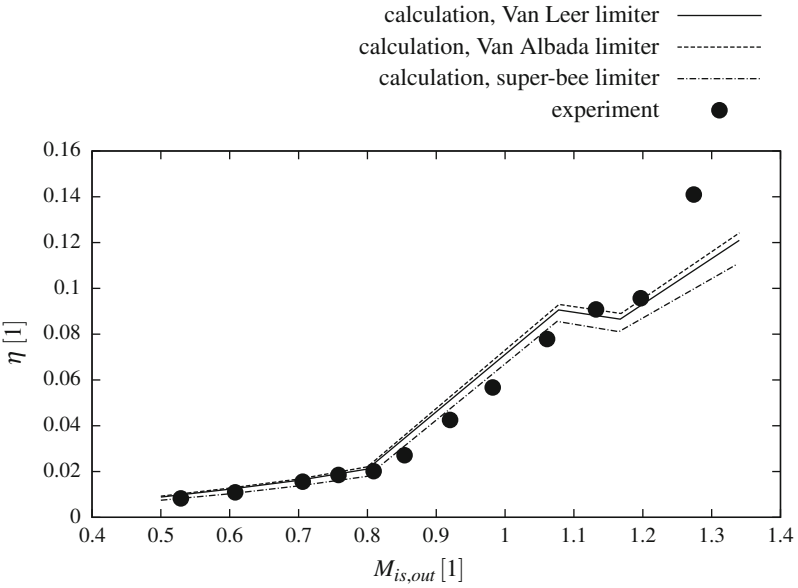

Fig. 7 Distribution of the total pressure loss coefficient

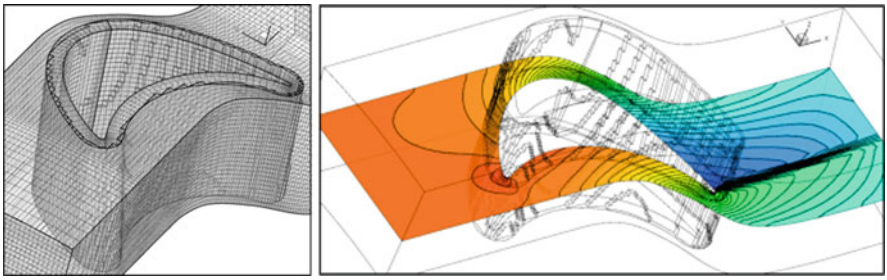

Fig. 8 Chimera mesh and the pressure distribution in 3D problem

4.1 Extension for 3D problem

It is simple to extend the method described in sec. 3 for 3D problems. Two-blocks structured chimera mesh with the hexahedral elements was used for solution of 3D transonic inviscid flow (described by Euler equation: $\frac{\partial \mathbf{W}}{\partial t} + \frac{\partial \mathbf{F}_i^{inv}}{\partial x_i}$, where $\mathbf{W} = [\rho, \rho u_1, \rho u_2, \rho u_3, e]^{\mathrm{T}}$ and $\mathbf{F}_i^{inv}$ $(i = 1, 2, 3)$ stands for inviscid flux vector) in an axial tubine cascade ST6 [8] for isentropic output Mach number $M_{is,out} = 1.3$, isentropic output Reynolds number $Re_{is,out} = 7.5 \times 10^5$ and angle of attack $\alpha = 45°$. Distribution of pressure is shown in Fig. 8.

5 Conclusion

The chimera mesh interface described in this contribution is simple for the implementation and robust for the transonic turbomachinery applications. Proposed method was applied for the calculation of transonic flow through the linear blade cascade VS33R. The results are in good agreement with the experimental data. Although the condition of conservation is not directly included in the chimera mesh interface, evaluation of the mass flux conservation error (Fig. 6) shows reasonably good conservation.

References

1. Kangle, X., Gang, S.: Assessment of an interface conservative algorithm MFBI in a chimera grid flow solver for multi-element airfoils. Proceedings of the World Congress on Engineering 2009 Vol II, London (2009)
2. Emmert, T., Lafon, P., Bailly, C.: Numerical study of self-induced transonic ow oscillations behind a sudden duct enlargement. Physics of Fluids, **21**, 106105 (2009)
3. Tang, H.S.: Chimera grid method for incompressible flows and its applications in actual problems. 10th Symposium on Overset Composite Grids and Solution Technology, NASA Ames Research Center, CA (2010)

4. Kok, J.C.: Resolving the dependence on freestream values for the $k - \omega$ turbulence model. AIAA Journal. **38**, 1292–1295 (2000)
5. Osher, S., Solomon, F.: Upwind diference schemes for hyperbolic system of conservation laws. Mathematics of Computation, **38**, 339-374 (1982)
6. Toro, E.F.: Riemann solvers and numerical methods for fluid dynamics, A practical introduction, 2nd edn. (Springer, Berlin, 1999)
7. Benetka, J., Kladrubský, M., Valenta, R., Vích, K.: Measurement of turbine blade cascade VS33R. Research report of Aeronautical research and test institute, R-3435/02, (Prague, 2002) (in Czech)
8. Straka, P.: Calculation of 3D unsteady inviscid flow in turbine stage ST6. Research report of Aeronautical research and test institute, R-4910, (Prague, 2010) (in Czech)

The paper is in final form and no similar paper has been or is being submitted elsewhere.